ChemComm

Development of GTP-responsive liposomes by exchanging the metal-DPA binding site in a synthetic lipid switch

Journal:	*ChemComm*
Manuscript ID	CC-COM-01-2023-000288.R1
Article Type:	Communication

COMMUNICATION

Development of GTP-responsive liposomes by exchanging the metal-DPA binding site in a synthetic lipid switch

Received 00th January 20xx,
Accepted 00th January 20xx

DOI: 10.1039/x0xx00000x

Jinchao Lou, †[a] Macy M. Hudson, †[a] Christelle F. Ancajas [a] and Michael D. Best *[a]

We report stimuli-responsive liposomes that selectively release encapsulated contents upon treatment with guanosine triphosphate (GTP) over a wide variety of phosphorylated metabolites, validated by fluorescence-based leakage assays. Significant changes in liposome self-assembly properties were also observed. Our results showcase the potential of this platform for triggered release applications.

Liposomes are spherical artificial nanocarriers composed of at least one lipid bilayer that are effective vehicles for drug delivery due to their biocompatibility and amphipathic characteristics that permit the encapsulation of a wide range of therapeutic cargo.[1] Additionally, liposomal platforms reduce off-target effects and toxicity while improving the solubility of encapsulated contests.[2] Due to these advantageous properties, an increasing number of liposomal therapeutics are in clinical use for biomedical applications.[3] In spite of this success, challenges remain that limit liposome therapeutic potential, particularly in terms of controlled release of cargo that is targeted to diseased cells. As a result, significant effort has gone into investigating liposome triggered release utilizing both active release that exploits externally supplied stimuli (*i.e.*, heat, ultrasound, and light)[4] and passive release that harnessing pathophysiological conditions (*i.e.*, redox environment, acidity, and enzyme expression).[5] Nevertheless, challenges remain for achieving stimuli-responsive liposomes in clinical application, especially since there are often only slight discrepancies between the conditions of healthy and diseased cells and delivering external stimuli can be toxic to healthy cells.

To overcome these challenges, recent efforts have targeted chemical species that are overly produced in diseased cells as the trigger for controlled content release from liposomes. This work benefits from insights gained from prior reports in the field. Early examples of synthetic lipid switches for triggered release commonly relied on modifying naturally existing non-bilayer lipids, such as 1,2-dioleoyl-*sn*-glycero-3-phosphoethanolamine (DOPE).[6] However, since DOPE generation only results in subtle changes to membrane properties, a high percentage of lipid switch is often required to induce significant membrane disruption, which is not ideal for clinical applications. To address this issue, synthetic lipid switches that undergo more substantial structural changes in the presence of chemical stimuli have emerged as powerful tools for triggering liposomal cargo release.[7] This approach was pioneered by the development of pH-responsive lipid switches designed to undergo dramatic conformational changes upon increases in acidity.[8] Building on that work, we reported metal ion-(calcium and zinc)[9] responsive liposomes driven by lipid switches that disrupt membrane packing upon metabolite binding through molecular recognition principles. Recently, we extended this approach by developing separate liposomal platforms that respond to adenosine 5'-triphosphate (ATP) and D-*myo*-inositol-1,4,5-triphosphate (IP_3),[10] demonstrating that liposomes can be directly triggered by small molecules as an expansion of toolbox for liposomal controlled release.

Herein, we report a modified lipid switch that gives rise to selective guanosine triphosphate (GTP)-responsive liposome properties. GTP is a crucial metabolite responsible for driving a multitude of intracellular enzymatic reactions as well as facilitating protein synthesis.[11] While intracellular GTP concentrations in healthy cells are in the range of 100-200 μM, GTP abundance in tumor cells is nearly 200% greater.[12] This overproduction arises since during protein synthesis, two molecules of GTP are consumed in order to incorporate a single amino acid into a growing polypeptide. Thus, rapidly dividing tumor cells require a significantly greater amount of GTP than healthy cells.[11] This variation in intracellular concentration

[a] *Department of Chemistry, University of Tennessee, Knoxville, TN, 37996, USA*
Email: mdbest@utk.edu
† Authors contributed equally
Electronic Supplementary Information (ESI) available: [details of any supplementary information available should be included here]. See DOI: 10.1039/x0xx00000x

renders GTP as a promising metabolite target for selective drug delivery to diseased cells.

The design of the current platform builds upon our ATP- and IP_3-responsive lipid switches, in which we mounted two or three, respectively, zinc(II) dipicolylamine (ZnDPA) recognition domains onto a rigid lipid scaffold.[10] This work showed that the binding of lipid switches to these specific metabolites induced conformational changes and triggered encapsulated content release. Metal chelated DPA units were selected since they exhibit high binding affinity toward different phosphorylated molecules.[13] While most work in the field of molecular sensing focused on ZnDPA, various reports have shown that switching the metal ion chelated to DPA can tune selectivity toward different phosphorylated metabolites.[10] For example, Yoon and co-workers reported a pyrophosphate (PPi)-selective fluorescent sensor containing a CuDPA binding site, while switching the metal center to zinc resulted in inactive probes.[14] Tian et al. reported a co-polymer containing DPA units that only showed diminished fluorescence upon Cu(II) addition, while Zn(II) did not induce any changes.[15] Additionally, in work unrelated to liposome release, copper nanoclusters have been reported as GTP sensors.[16] As a result, we hypothesized that swapping the metal ion chelated within a bis-DPA lipid switch scaffold to produce a bis-CuDPA lipid (**BCuDPAL**) could alter selectivity and potentially bind to GTP (Scheme 1). This compound is designed such that GTP binding will cause headgroups to constrict, leading to a cone-shaped lipid that disrupts membrane packing and induces cargo release.

The synthetic route to **BCuDPAL** (Scheme S1) simply entails production of precursor **1** as reported previously,[10a] followed by copper chelation. With this compound synthesized, we evaluated its ability to trigger release from liposomes using fluorescence-based dye release assays, initially using the hydrophobic dye Nile red (NR) as cargo. NR fluorescence is activated within the hydrophobic membrane environment but is quenched upon escape into the aqueous environment, which often leads to precipitation.[17] Thus, NR is as an effective hydrophobic drug mimic and provides fluorescence changes needed for detection. These experiments employed unilamellar liposomes composed primarily of L-α-phosphatidylcholine (PC, mixed isomer from egg), which was doped with **BCuDPAL** (10%, 15%, 20% or 25%) and NR. Liposomes were prepared using a thin-film hydration protocol including film preparation, hydration, freeze-thaw cycling, and extrusion through 200 nm membranes. Successful liposome formation was proven by dynamic light scattering (DLS) analysis, as will be discussed later in the context of liposome size changes driven by GTP binding.

The selectivity of metabolite-driven NR release from liposomes (2 mM) was screened using a panel of phosphorylated metabolites including sodium phosphate (Pi), PPi, adenosine 5'-diphosphate (ADP), ATP, D-Fructose-6-phosphate (FP), D-fructose-1,6-bisphosphate (FBP), adenosine 5'-monophosphate (AMP), sodium tripolyphosphate (TPi), cytidine-5'-triphosphate (CTP), GTP, uridine 5'-triphosphate (UTP) and IP_3. After an initial scan, each analyte was added to the cuvette to produce a final concentration of 5 mM. Following incubation with liposomes for 1 hour, another reading was taken. For 20% **BCuDPAL**/PC liposomes**,** which showed the greatest activity, among the metabolites tested only GTP incubation resulted in a significant decrease in NR fluorescence (~40%, Figure 1). TPi and PPi resulted in an increase in NR fluorescence, which could possibly be explained by binding of TPi/PPi to **BCuDPAL** in a manner that altered the membrane microenvironment to enhance NR fluorescence. Negative control experiments were carried out by either subjecting liposomes lacking **BCuDPAL** (100% PC) to each metabolite or treating 20% **BCuDPAL**/PC liposomes with Milli-Q purified water (MQ), both of which exhibited minimal fluorescence changes. Interestingly, liposomes with reduced **BCuDPAL** (10%, replaced by PC), did not show NR decrease upon treatment with any of these metabolites. This is in line with prior observations that activity and selectivity is dependent on the percentage of lipid switch included within the liposome.[10a] For 15% and 25% **BCuDPAL**/PC liposomes (Figure S1), while GTP treatment resulted in the greatest decrease (~20%) in NR fluorescence, 25% liposomes released cargo upon ATP, GTP, UTP and IP_3 addition, diminishing selectivity. This is further demonstrated by pictures taken for liposomes before and after analyte treatment (Figure S2). These results demonstrate that 20% **BCuDPAL**/PC liposomes show excellent selectivity toward GTP among other common phosphorylated metabolites. Additionally, doping of **BCuDPAL** into the bilayer lipid PC was

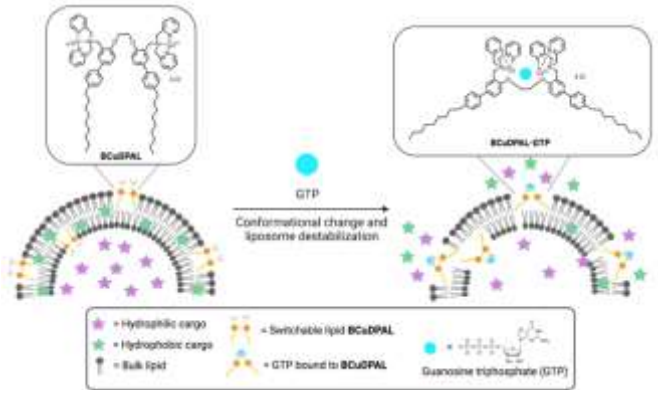

Scheme 1. Structure of **BCuDPAL** and cartoon depicting liposome triggered release driven by GTP binding. **BCuDPAL** is designed to initially adopt a cylindrical shape to maintain a stable membrane. GTP treatment is expected to induce a conformational change that disrupts bilayer integrity and triggers liposomal content release.

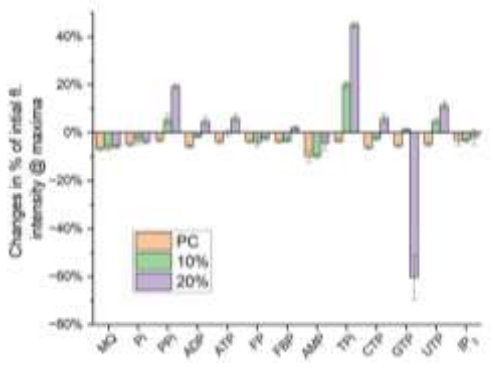

Figure 1. NR release selectivity screen by treating 0%, 10%, or 20% **BCuDPAL**/PC with different phosphorylated metabolites. A significant decrease in NR fluorescence was only observed for 20% **BCuDPAL**/PC liposomes upon 5 mM GTP incubation, while PC or 10% **BCuDPAL**/PC liposomes showed minimal changes after analyte treatments. Error bars denote standard errors from at least three independent studies.

alone sufficient for driving GTP-responsive properties without requiring non-bilayer additives such as DOPE that are often needed to destabilize the bilayer and prime liposomes for release.

We next explored changes to liposome self-assembly properties concomitant with triggered release using DLS. The particle sizes of 0%, 10%, 15%, 20% or 25% **BCuDPAL**/PC liposomes before and after the addition of each metabolite were measured (Figures 2 and S4A). All liposomes before analyte treatment showed uniform sizes (~150 nm) in the range expected following extrusion using 200 nm membranes. Significant particle size increases were observed for 20% **BCuDPAL**/PC liposomes after 5 mM GTP treatment. Of note is that changes in average particle sizes were not observed with TPi and PPi, which had yielded fluorescence increases in NR screens, underscoring that these analytes don't appear to modulate liposomal properties. While 15% liposomes only exhibited size changes upon GTP treatment, addition of ATP, TPi, GTP, UTP and IP_3 all resulted in larger particles for 25% liposomes. Changes in polydispersity indices (PDIs) of the samples were similar (Figures S3 and S4B); 20% **BCuDPAL**/PC liposomes only exhibited a dramatic increase in PDI after GTP treatment, further supporting membrane disruption. Raw DLS distribution curves (Figure S5) and corresponding Z-average and PDI values (Table S1) are also included. These results showcase that changes in liposome properties only occurred upon GTP treatment and that the percentage of **BCuDPAL** (i.e., 15%) beyond a threshold is required to observe these effects. In addition, the selectivity of the liposomes toward GTP can be tuned by adjusting **BCuDPAL** lipid incorporation.

GTP-driven morphology changes can be explained by liposome fusion or lipid reorganization triggered by membrane disruption resulting from metabolite binding, both of which could lead to increases in particle sizes. To further explore this, we conducted fluorescence microscopy studies to visualize the formation of larger aggregates over time.[10a] We prepared 1 mM 0% or 20% **BCuDPAL**/PC liposomes labeled with 0.08% of the fluorescent lipid rhodamine L-α-phosphatidylethanolamine (Rd-PE). These liposomes were imaged before and after addition of 0.5 mM GTP under a confocal fluorescence microscope. Both sets of initial liposomes show minimal fluorescence under the microscope due to resolution limits (Figure S6). After 15 minutes of GTP incubation, highly fluorescent particles with

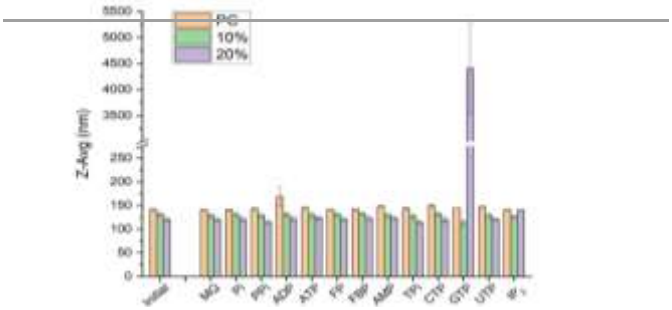

Figure 2. DLS analysis of 0%, 10%, and 20% **BCuDPAL**/PC liposomes before and after metabolites. Initial liposomes showed uniformly size particles of desired diameters. GTP addition to 20% **BCuDPAL**/PC liposomes resulted in dramatic increases in average particle sizes, while all other formulation/analyte combinations showed minimal diameters in the micrometer range were observed for 20% **BCuDPAL**/PC liposomes. In contrast, the image for PC liposomes remained dim, which was supported by bright field images. It is worth noting that while NR release experiments required 5 mM GTP treatment, a significantly lower amount of GTP (0.5 mM) was sufficient to observe particle changes in this experiment. Time-course videos are included to show the formation of fluorescent aggregates over time (Videos S1-2).

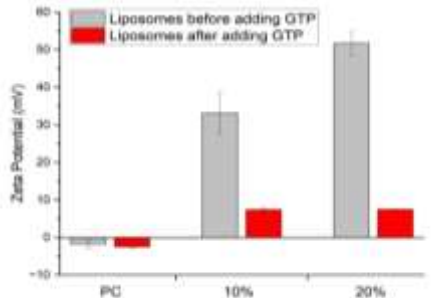

Figure 3. Zeta potential analysis for 0%, 10%, or 20% **BCuDPAL**/PC liposomes before and after GTP. Positively charged 10% and 20% **BCuDPAL**/PC liposomes showed reductions in positive charge upon GTP addition. PC control liposomes showed only minimal ZP changes after GTP. Error bars denote standard errors from at least three independent

We next set out to confirm that **BCuDPAL** liposomes bind GTP using zeta potential analysis as a measure of particle surface charge. **BCuDPAL** liposomes (0%, 10%, or 20% in PC) were prepared and their zeta potential values were measured before and after GTP treatment. Both 10% and 20% **BCuDPAL**/PC liposomes were initially highly positively charged due to the presence of two copper ions per **BCuDPAL** (Figure 3). After GTP treatment, both showed a dramatic decrease in surface charge indicating the binding of the negatively charged GTP to the membrane. PC control liposomes were slightly negatively charged, in agreement with previous reports,[18] and the addition of GTP did not significantly alter their surface charge. These results support that **BCuDPAL** binds to GTP within the membrane environment during the release process.

Liposomes are also capable of encapsulating and delivering hydrophilic cargo, a prominent characteristic considering recent advances in RNA-based therapeutics, including COVID-19 vaccines in which lipid nanoparticles encapsulate mRNA sequences.[19] To evaluate polar content release, we employed the hydrophilic fluorescent dye calcein, for which fluorescence can be quenched at high concentrations within liposomes, and dye leakage restores fluorescence by deactivating collisional quenching.[20] In this case, liposomes were subjected to size-exclusion chromatography (SEC) following extrusion to remove unencapsulated dye. The successful formation of liposomes was proven by DLS (Figure S7, raw distribution curve in Figure S8).

We first performed titration experiments through incremental addition of GTP to either 100% PC or 20% **BCuDPAL**/PC liposomes (Figure S9). At the end of each experiment, Triton X-100 was added to lyse liposomes and obtain a reference to which each point was compared by converting data into percent of total release. A dose-dependent increase in fluorescence was observed for 20% **BCuDPAL**/PC liposomes upon GTP treatment. The titration curve exhibited an induction period requiring ~5-6 mM GTP, after which further

GTP resulted in significant signal increase, which plateaued after ~15 mM GTP treatment (~80% release). PC control liposomes resulted in ~10% change from non-specific leakage. Dilution effects were accounted for by additional control experiments where Milli-Q purified water was titrated into liposome samples and the resulting fluorescence decreases were subtracted out. We next performed kinetic experiments by adding 10 mM GTP to 0% or 20% **BCuDPAL**/PC liposomes and acquiring fluorescence readings over time. For 20% **BCuDPAL**/PC liposomes, a dramatic increase in calcein fluorescence (~40%) was observed immediately after adding GTP (Figure 4), which plateaued after 10 minutes. Meanwhile, PC control liposomes only exhibited minimal background leakage (~10%). A representative kinetic curve is shown in Figure S10. Morphology changes were also detected during hydrophilic cargo release by DLS (Figures S7 and S8), in which uniform particles for 20% **BCuDPAL**/PC liposomes of ~150 nm transitioned into larger aggregations with GTP treatment, while PC control liposomes remained the same. These results indicate that liposomes containing **BCuDPAL** effectively drive release of hydrophilic cargo from liposomes upon GTP treatment. It should be acknowledged that physiological concentrations for GTP in tumor cells (< 0.4 mM) are lower than those that yield release in this platform (~5 mM). Nevertheless, the current work is an initial advancement toward the goal of drug delivery mediated by disease-related metabolite concentrations.

In conclusion, we have successfully developed a liposomal triggered release platform in which **BCuDPAL** enables release of both hydrophilic and hydrophobic cargo upon GTP treatment among a panel of various phosphorylated metabolites. While further cellular delivery studies are desired, this work further demonstrates that molecular recognition events between disease-associated metabolites and rationally designed lipid switches can be harnessed to expand the toolbox for stimuli-responsive liposome development. Furthermore, this system shows that modular lipid switch scaffolds can be repurposed by altering features such as metal chelation sites to reprogram the selectivity of metabolite-responsive properties. We envision that other biomolecules that are upregulated in disease states can be explored using a similar strategy.

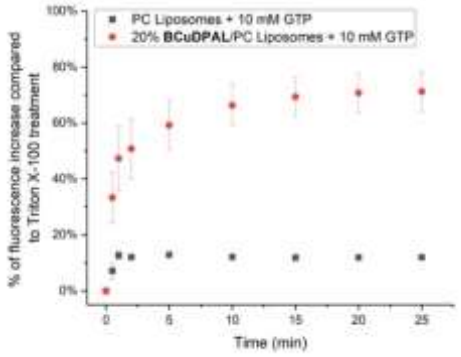

Figure 4. Time-dependent calcein release for PC and 20% **BCuDPAL**/PC liposomes after adding 10 mM GTP. More than ~70% release was observed within 10 min. Data indicate percentages of fluorescence increases relative to maximum release using Triton X-100. Error bars denote standard errors from at least three independent studies.

This material is based upon work supported by the National Science Foundation under grant DMR-1807689. We thank Dr. Michael D. Pluth for helpful discussions.

Conflicts of interest

There are no conflicts to declare.

Notes and references

1. A. Akbarzadeh, R. Rezaei-Sadabady, S. Davaran, S. W. Joo, N. Zarghami, Y. Hanifehpour, M. Samiei, M. Kouhi and K. Nejati-Koshki, *Nanoscale Res. Lett.*, 2013, **8**, 1.
2. B. S. Pattni, V. V. Chupin and V. P. Torchilin, *Chem. Rev.*, 2015, **115**, 10938.
3. N. Filipczak, J. Pan, S. S. K. Yalamarty and V. P. Torchilin, *Adv. Drug Deliv. Rev.*, 2020, **156**, 4.
4. E. Yuba, *J. Mater. Chem. B*, 2020, **8**, 1093.
5. a) A. Raza, U. Hayat, T. Rasheed, M. Bilal and H. M. N. Iqbal, *Eur. J. Med. Chem.*, 2018, **157**, 705; b) J. Lou and M. D. Best, *Bioconjugate Chem.*, 2020, **31**, 2220; c) N. M. AlSawaftah, N. S. Awad, W. G. Pitt and G. A. Husseini, *Polymers*, 2022, **14**, 936; d) F. Fouladi, K. J. Steffen and S. Mallik, *Bioconjugate Chem.*, 2017, **28**, 857; e) J. Lou and M. D. Best, *Chem. Eur. J.*, 2020, **26**, 8597.
6. a) J. N. Israelachvili, D. J. Mitchell and B. W. Ninham, *Biochim. Biophys. Acta, Biomembr.*, 1977, **470**, 185; b) J. Lou and M. D. Best, *Chem. Phys. Lipids*, 2020, **232**, 104966.
7. a) J. Lou, X. Zhang and M. D. Best, *Chem. Eur. J.*, 2019, **25**, 20; b) J. Lou, R. Sagar and M. D. Best, *Acc. Chem. Res.*, 2022, **55**, 2882.
8. a) W. Viricel, A. Mbarek and J. Leblond, *Angew. Chem. Int. Ed. Engl.*, 2015, **54**, 12743; b) B. Brazdova, N. Zhang, V. V. Samoshin and X. Guo, *Chem. Commun.*, 2008, 4774.
9. a) J. Lou, A. J. Carr, A. J. Watson, S. I. Mattern-Schain and M. D. Best, *Chem. Eur. J.*, 2018, **24**, 3599; b) R. Sagar, J. Lou, A. J. Watson and M. D. Best, *Bioconjugate Chem.*, 2021, **32**, 2485.
10. a) J. Lou, J. A. Schuster, F. N. Barrera and M. D. Best, *J. Am. Chem. Soc.*, 2022, **144**, 3746; b) S. E. Bottcher, J. Lou and M. D. Best, *Chem. Commun.*, 2022, **58**, 4520.
11. K. Sumita, Y. H. Lo, K. Takeuchi, M. Senda, S. Kofuji, Y. Ikeda, J. Terakawa, M. Sasaki, H. Yoshino, N. Majd, et al., *Mol. Cell*, 2016, **61**, 187.
12. D. Zala, U. Schlattner, T. Desvignes, J. Bobe, A. Roux, P. Chavrier and M. Boissan, *F1000Res.*, 2017, **6**, 724.
13. a) H. T. Ngo, X. Liu and K. A. Jolliffe, *Chem. Soc. Rev.*, 2012, **41**, 4928; b) J. A. Drewry and P. T. Gunning, *Coord. Chem. Rev.*, 2011, **255**, 459; c) S. Anbu, A. Paul, G. J. Stasiuk and A. J. Pombeiro, *Coord. Chem. Rev.*, 2021, **431**, 213744.
14. M. J. Kim, K. M. Swamy, K. M. Lee, A. R. Jagdale, Y. Kim, S. J. Kim, K. H. Yoo and J. Yoon, *Chem. Commun.*, 2009, , 7215.
15. Z. Guo, W. Zhu and H. Tian, *Macromolecules*, 2010, **43**, 739.
16. X. J. Zhao and C. Z. Huang, *New J. Chem.*, 2014, **38**, 3673.
17. a) P. Greenspan, E. P. Mayer and S. D. Fowler, *J. Cell. Biol.*, 1985, **100**, 965; b) X. Liang, X. Yue, Z. Dai and J.-i. Kikuchi, *Chem. Commun.*, 2011, **47**, 4751.
18. D. G. Fatouros and S. G. Antimisiaris, *J. Colloid Interface Sci.*, 2002, **251**, 271.
19. a) B. Ozpolat, A. K. Sood and G. Lopez-Berestein, *Adv. Drug Deliv. Rev.*, 2014, **66**, 110; b) Y. Eygeris, M. Gupta, J. Kim and G. Sahay, *Acc. Chem. Res.*, 2021, **55**, 2.
20. T. Allen, in *Liposome Technology*, CRC press, 2018, pp. 177.